

# ChemPhysChem

Supporting Information

## **3D Printable Polymer Electrolytes for Ionic Conduction based on Protic Ionic Liquids**

Alyna Lange,\* Sajal Arwish, Aurelie Rensonnet, Khalid Elamin, Iqbaal Abdurrokhman, Zaneta Wojnarowska, Mark Rosenwinkel, Cedric Malherbe, Monika Schönhoff, Kerstin Zehbe, and Andreas Taubert\*

## 3D Printable Polymer Electrolytes for Ionic Conduction based on Protic Ionic Liquids

Alyna Lange<sup>1\*</sup>, Sajal Arwish<sup>2</sup>, Aurelie Rensonnet<sup>3</sup>, Khalid Elamin<sup>4</sup>, Iqbaal Abdurrokhman<sup>4</sup>, Zaneta Wojnarowska<sup>5</sup>, Mark Rosenwinkel<sup>2</sup>, Cedric Malherbe<sup>3</sup>, Monika Schönhoff<sup>2</sup>, Kerstin Zehbe<sup>1</sup>, Andreas Taubert<sup>1\*</sup>

### 1. Batch reproducibility

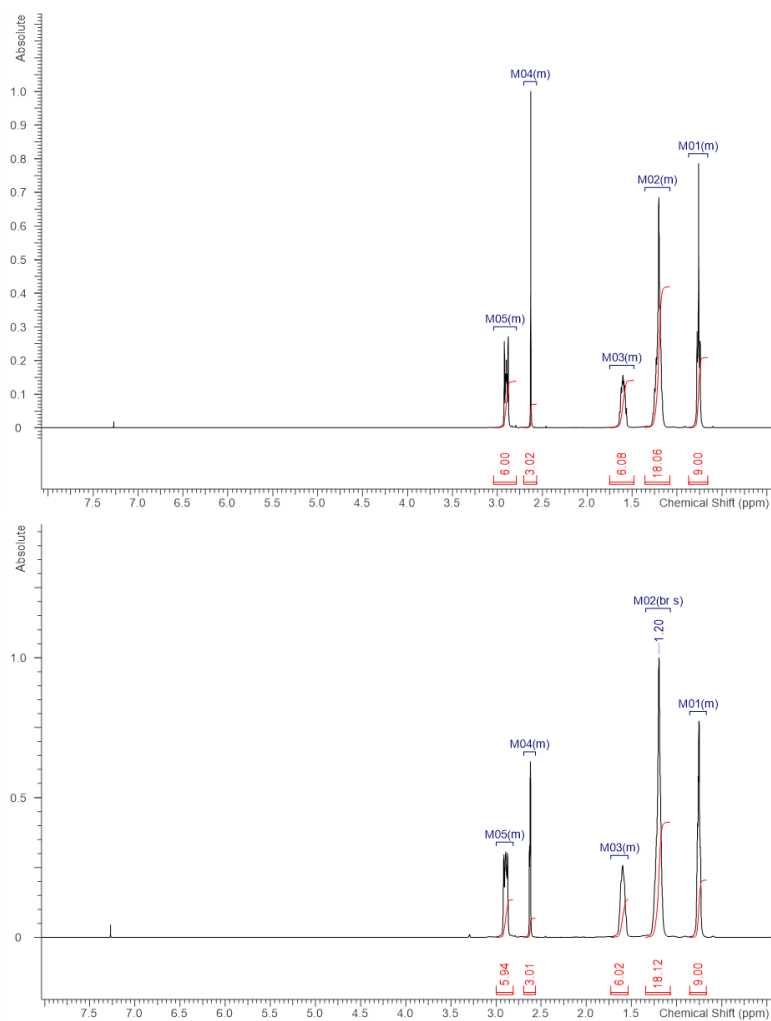
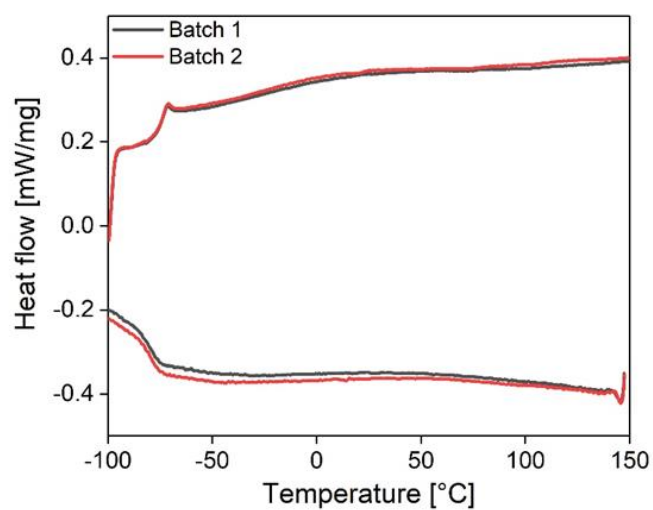
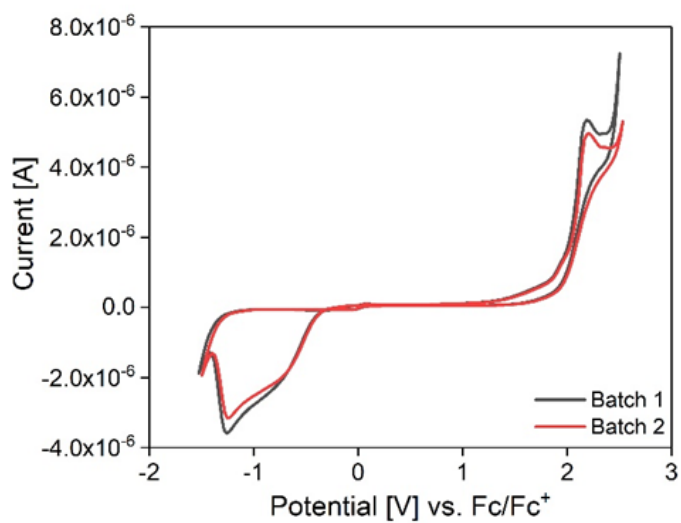


Figure S1: <sup>1</sup>H-NMR spectra for two different THMS batches.



**Figure S2:** 2<sup>nd</sup> heating and cooling DSC runs for two different THMS batches.



**Figure S3:** CV curves for two different THMS batches.

## 2. Ionogel images

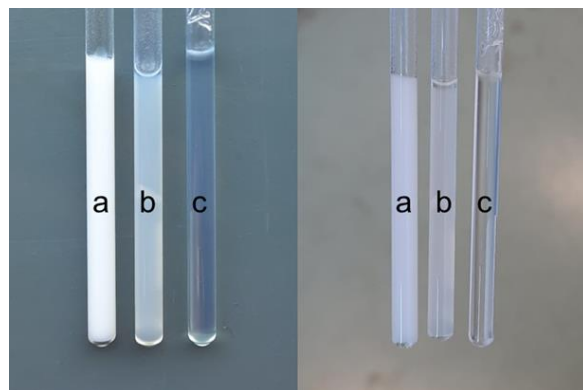


**Figure S4:** Representative pictures of selected IGs with different compatibilities: a) poor compatibility (TOOTf), b) limited compatibility (THOTf) and c) good compatibility (THMS).

## 3. Thermal data for ILs and IGs

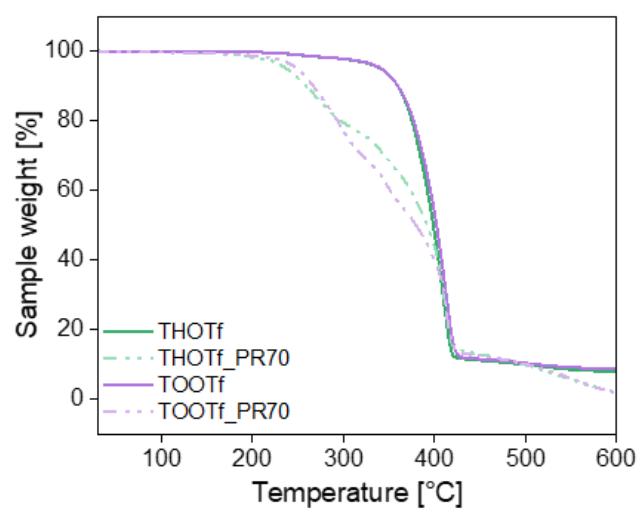


**Figure S5:** TGA curves for fluorinated ILs and IGs.

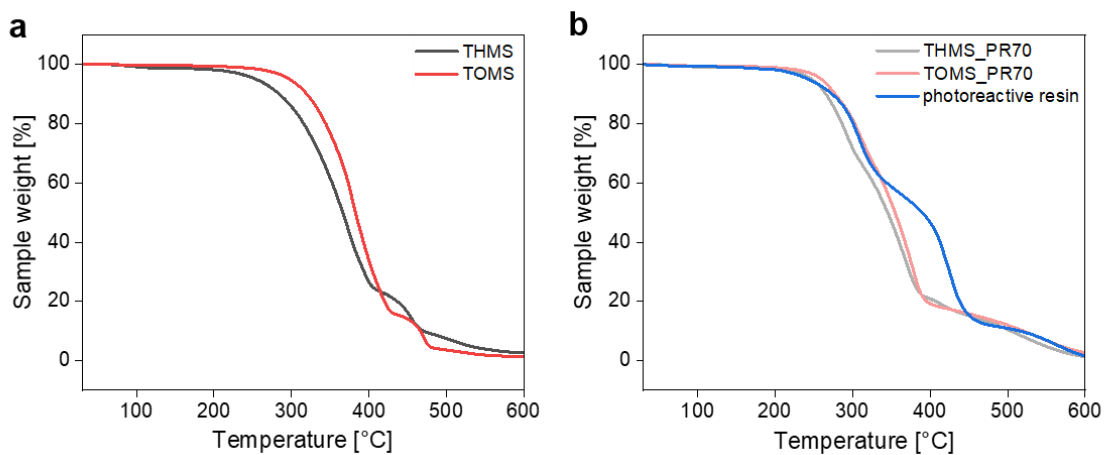


**Figure S6:** TGA curves for a) mesylate based ILs, b) mesylate based IGs and resin.

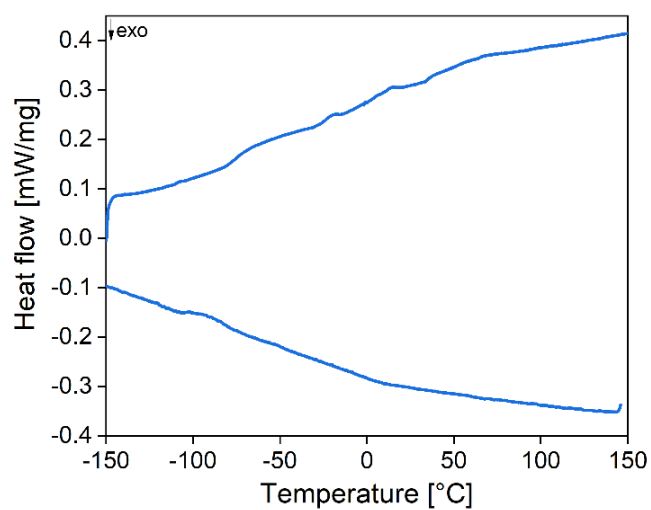


**Figure S7:** 2<sup>nd</sup> heating and cooling DSC runs for photoreactive resin.

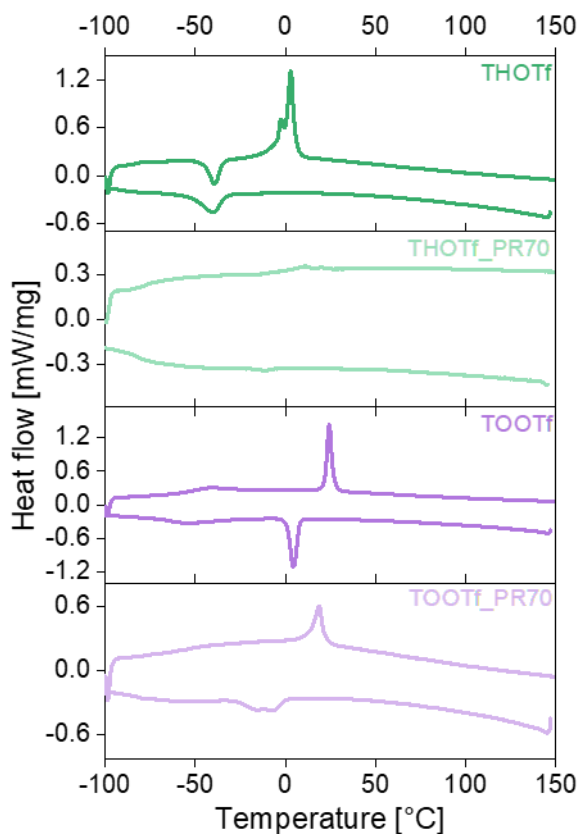


**Figure S8:** 2<sup>nd</sup> heating and cooling DSC runs for fluorinated ILs and IGs.

#### 4. Detailed IR discussion

**ILs:** Bands in the range between 1470-1300  $\text{cm}^{-1}$  can originate from different vibrations such as C-C- and N-C<sub>3</sub>-asymmetric stretching or R-CH<sub>2</sub>-R- and CH<sub>3</sub>-bending. The pronounced bands between 1240-1140 arise from SO<sub>3</sub>-asymmetric stretching and therefore show the presence of sulfonate groups. These can also be identified via the SO<sub>3</sub>-symmetric stretching bands at 1040-1030  $\text{cm}^{-1}$  and the SO<sub>3</sub>-bending vibrations between 550-520  $\text{cm}^{-1}$ . The presence of both methanesulfonate and trialkylammonium in the ILs is also confirmed by the presence of bands between 760-720  $\text{cm}^{-1}$ . These can be assigned to C-S-stretching and N-C<sub>3</sub>-symmetric stretching vibrations.<sup>1</sup>

**IGs:** The broad band at 3430  $\text{cm}^{-1}$  is probably an overlapping signal from N-H- and O-H-vibrations, where the N-H-stretching vibrations originate from the polymer and the O-H-stretching vibrations from possible water uptake of the IG or interactions between polymer and IL. The band at 1730  $\text{cm}^{-1}$  shows the presence of carbonyl groups via C=O-vibration. The band at 1540  $\text{cm}^{-1}$  can be attributed to C-N-H bending and the band around 1370  $\text{cm}^{-1}$  to C-N-stretching and C-H-bending/rocking vibrations. The presence of asymmetric C-O-C- and C-N-C-stretching vibrations originating in the acrylate- and urethane nature of the polymer-mixture can be seen in the pronounced band around 1110  $\text{cm}^{-1}$ . Small bands around 1000  $\text{cm}^{-1}$  can be attributed to symmetric C-O-C-stretching vibrations.<sup>1-4</sup> The characteristic bands between 1480-1440  $\text{cm}^{-1}$  and 1230-1190  $\text{cm}^{-1}$ , which can be associated with CH<sub>2</sub> and O-CH<sub>3</sub> bending and C-O stretching vibrations in the pure polymer resin cannot be observed clearly in the IGs, because they overlap with other bands from the ILs.

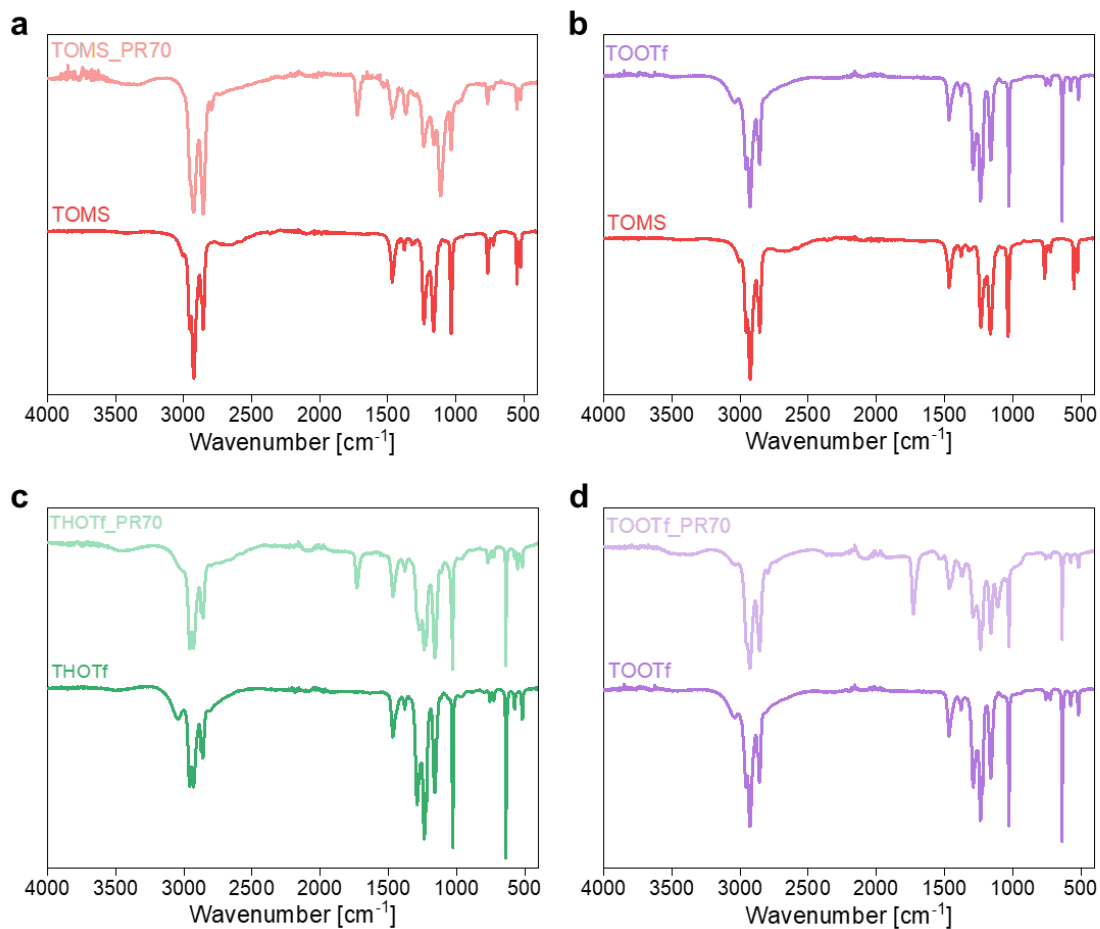


**Figure S9:** IR spectra; a) TOMS and IG, b) comparison trioctyl-based ILs, c) THOTf and IG, d) TOOTf and IG.

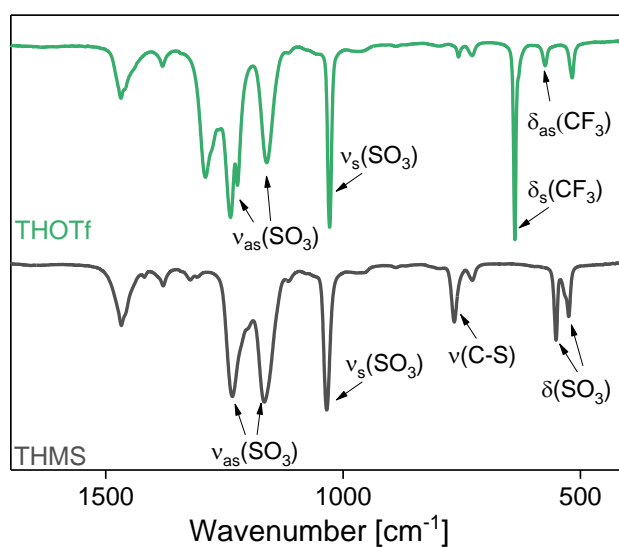


**Figure S10:** Fingerprint area of IR spectra for THMS and THOTf.

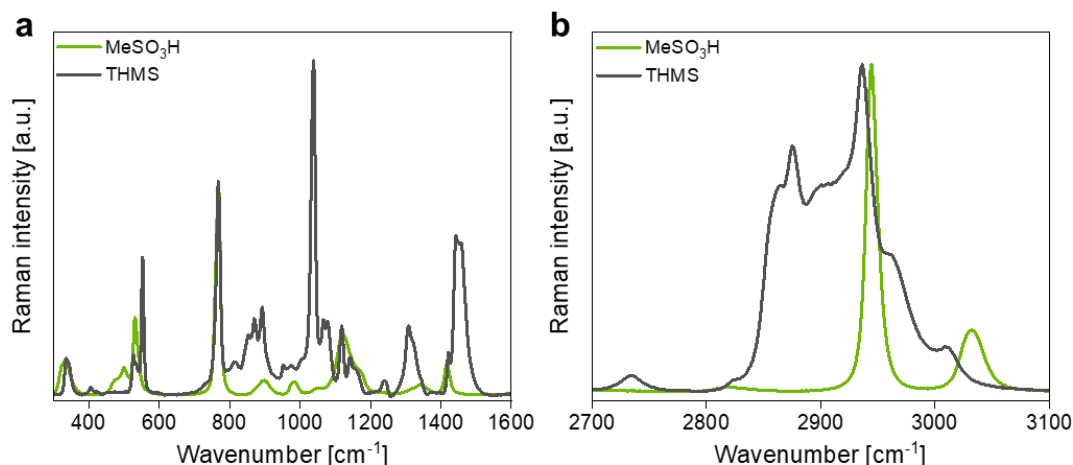


**Figure S11:** Raman spectra of THMS and pure methanesulfonic acid in a) low wavenumber region, and b) high wavenumber region.

**Table S1:** Raman shifts and assignments for THMS and TOMS.

Raman shift [cm <sup>-1</sup> ]		Assignment
THMS	TOMS	
340	340	SO <sub>3</sub> rocking <sup>5,6</sup>
530, 553	530, 553	SO <sub>3</sub> bending <sup>5,6,9</sup>
768	768	C-S stretching <sup>5,6,9</sup>
813, 851, 871, 892, 953	810, 846, 872, 891, 926, 958	C-C, C-N stretching, CH <sub>2</sub> /CH <sub>3</sub> rocking <sup>7,8,9</sup>
1038	1039	SO <sub>3</sub> stretching <sup>5,6,9</sup>
1066, 1080	1063, 1081	
1118	1122	SO <sub>3</sub> stretching <sup>9</sup>
1141, 1159	1139, 1153	C-N stretching <sup>9</sup>
1307, 1315	1304, 1319	CH <sub>2</sub> /CH <sub>3</sub> scissoring <sup>7,8</sup>
1421	1420	CH <sub>3</sub> bending (anion) <sup>5,6,9</sup>
1441, 1451	1439, 1453	CH <sub>3</sub> /CH <sub>2</sub> bending <sup>7,8,9</sup>
2859	2855	Symmetric CH <sub>2</sub> stretching <sup>9,10</sup>
2876, 2895	2875, 2894	Symmetric CH <sub>3</sub> stretching <sup>9,10</sup>
2917	2913	Asymmetric CH <sub>2</sub> stretching <sup>9,10</sup>
2937, 2962	2937, 2962	Asymmetric CH <sub>3</sub> stretching <sup>9,10</sup>
3009	3009	Asymmetric N-H stretching <sup>9</sup>

**Table S2:** Raman shifts and assignments for pure MeSO<sub>3</sub>H acid.

Raman shift [cm <sup>-1</sup> ]	Assignment*
333	SO <sub>3</sub> rocking <sup>5,6</sup>
479	SO <sub>3</sub> bending <sup>5</sup>
501	SO <sub>3</sub> bending <sup>5</sup>
532	SO <sub>3</sub> bending <sup>5,6</sup>
767	C-S stretching <sup>5,6</sup>
897	S-OH stretching <sup>5</sup>
983	CH <sub>3</sub> rocking <sup>5,6</sup>
1122	SO <sub>3</sub> stretching <sup>5</sup>
1164	O-H bending <sup>5</sup>
1340	SO <sub>3</sub> stretching <sup>5</sup>
1418	CH <sub>3</sub> bending <sup>5,6</sup>
2945	Symmetric CH <sub>3</sub> stretching <sup>5,6</sup>
3033	Asymmetric CH <sub>3</sub> stretching <sup>5,6</sup>

\*We find that there is evidence of hydrogen bonding within the molecules of methanesulfonic acid. Therefore, due to this intermolecular bonding, the three oxygen atoms become equivalent, which is why we refer the attribution to the SO<sub>3</sub> group instead of SO<sub>2</sub>.

## 5. Electrochemical analysis

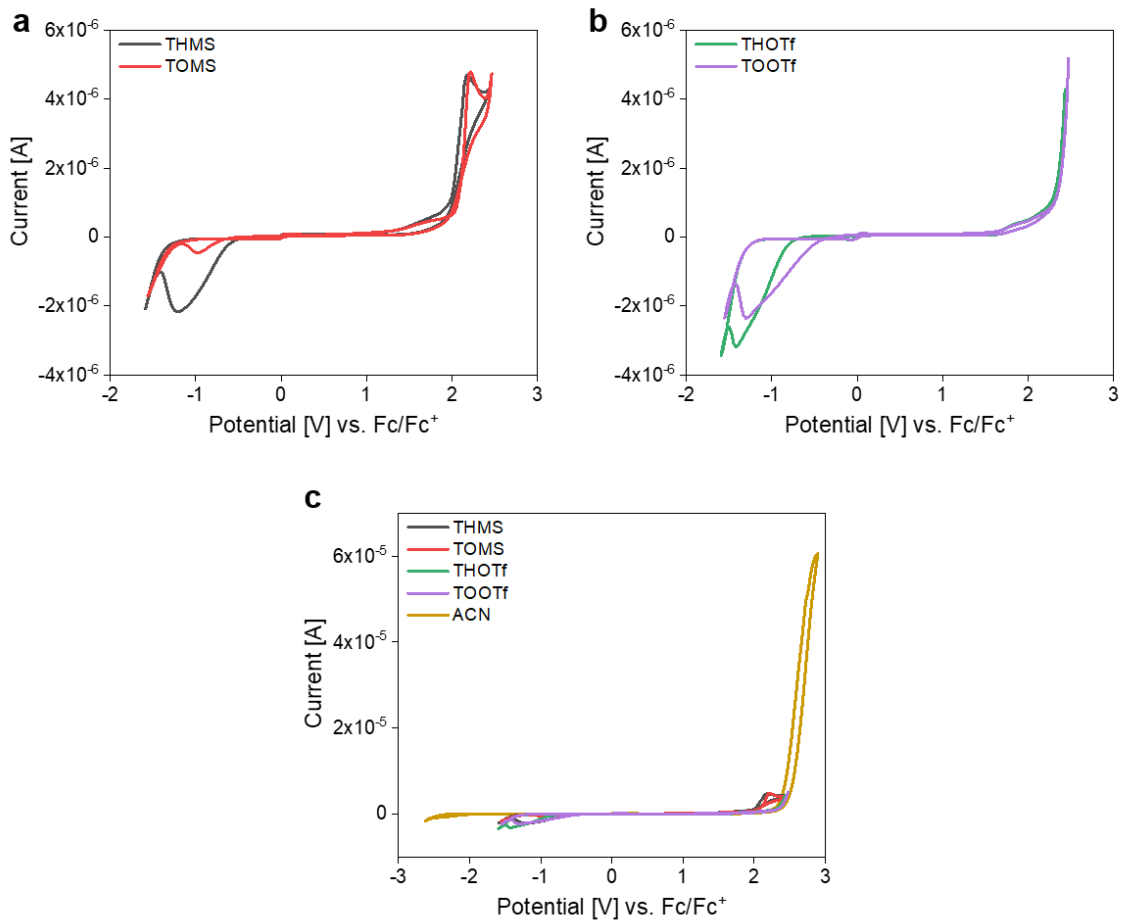


**Figure S12:** CV curves for a) protonated ILs, b) fluorinated ILs, c) all ILs and solvent (ACN).

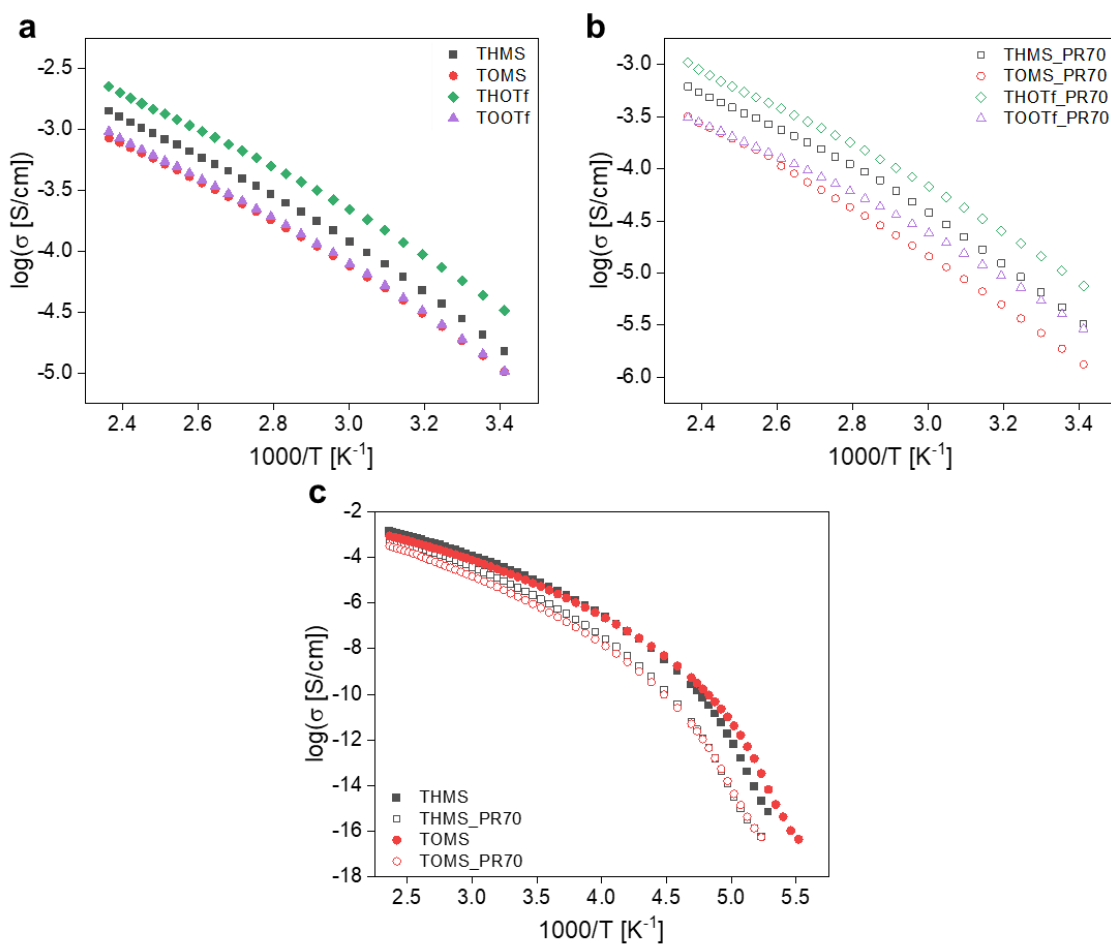


**Figure S13:** Ionic conductivities for a) pure ILs, b) IGs and c) protonated compounds until  $T_g$ .

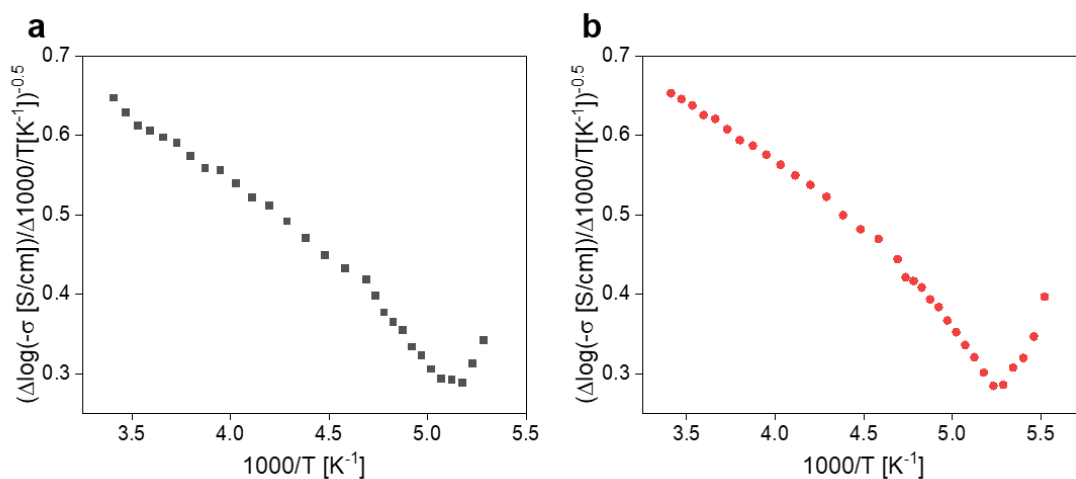


**Figure S14:** Representative Stickel plots for a) THMS and b) TOMS.

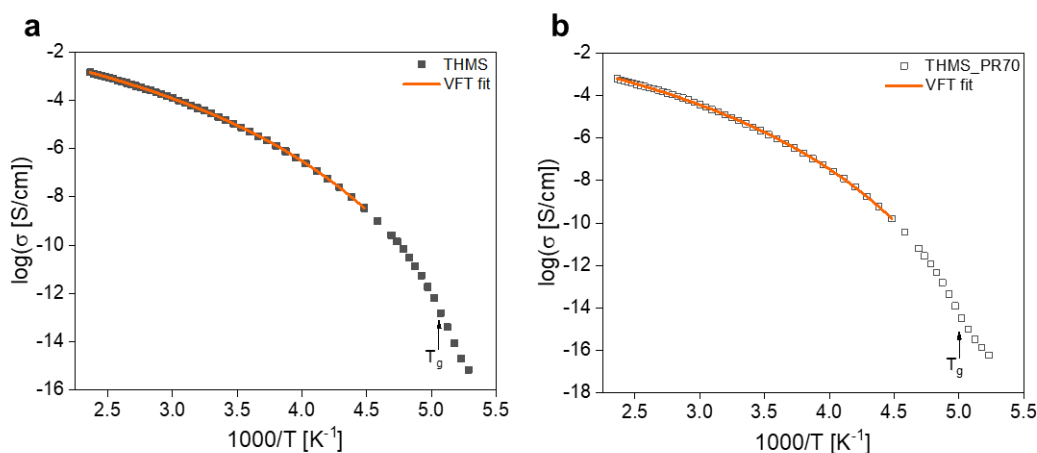


**Figure S15:** Representative VFT Fits for conductivities of a) THMS and b) THMS\_PR70. The graphs were hereby fitted to the data points above  $4.5 \text{ K}^{-1}$  to stay well above the glass transition.

**VFT fit:** The graphs were hereby fitted to the data points above  $4.5 \text{ K}^{-1}$  (mesylate based compounds) and  $3.4 \text{ K}^{-1}$  (triflate based compounds) to stay above glass transition or crystallization processes.

## 6. IL densities

**Table S3:** Densities of pure ILs at  $60 \text{ }^\circ\text{C}$ .

	Density $\rho$ [g/mL]
<b>THMS</b>	0.9341
<b>TOMS</b>	0.9080
<b>THOTf</b>	1.0138
<b>TOOTf</b>	0.9738

## References

- (1) Larkin, P. *Infrared and Raman Spectroscopy: Principles and Spectral Interpretation*; Elsevier, **2018**.
- (2) Cui, J. Synthesis of UV-Cured Hyperbranched Polyurethane Acrylate Coatings and Its Corrosion Resistance Revealed by Electrochemistry. *Int. J. Electrochem. Sci.* **2016**, 3727–3737.
- (3) Mashouf, G.; Ebrahimi, M.; Bastani, S. UV curable urethane acrylate coatings formulation: experimental design approach. *Pigment & Resin Technology* **2014**, 43, 61–68.
- (4) Dapawan Kunwong, Natthawadee Sumanochitraporn, S. Kaewpirom. Curing behavior of a UV-curable coating based on urethane acrylate oligomer: the influence of reactive monomers. *Songklanakarinn J. Sci. Technol.*, **2011**, 201–207.
- (5) Zhong, L.; Parker, S. F. R. Soc. open sci. 2018, 5 (12), 181363.
- (6) Capwell, R. J.; Rhee, K. H.; Seshadri, K. S. *Spectrochimica Acta Part A: Molecular Spectroscopy*. 1968, 24 (8), 955–958.

- (7) Bodo, E.; Mangialardo, S.; Ramondo, F.; Ceccacci, F.; Postorino, P. J. *Phys. Chem. B.* 2012, 116 (47), 13878–13888.
- (8) Paschoal, V. H.; Faria, L. F. O.; Ribeiro, M. C. C. *Chem. Rev.* 2017, 117 (10), 7053–7112.
- (9) Pan, H.; Geysens, P.; Putzeys, T.; Gennaro, A.; Yi, Y.; Li, H.; Atkin, R.; Binnemans, K.; Luo, J.; Wübbenhorst, M. *The Journal of Chemical Physics.* 2020, 152 (23), 234504.
- (10) Howell, N. K.; Arteaga, G.; Nakai, S.; Li-Chan, E. C. Y. *J. Agric. Food Chem.* 1999, 47 (3), 924–933.